

Supporting Information

Theoretical Investigation of Lanthanides and Actinides Encapsulated $M@Pb_{12}^{2-}$ and $M@Sn_{12}^{2-}$ Zintl Clusters ($M = Lr^n, Lu^n, La^{3+}, Ac^{3+}$ and $n = 0, 1, 2, 3$)

Meenakshi Joshi^{†,‡}, Aditi Chandrasekar^{‡,§} and Tapan K. Ghanty^{†,‡,*}

[†]*Theoretical Chemistry Section, Chemistry Group, Bhabha Atomic Research Centre,
Mumbai 400 085, INDIA.*

[‡]*Homi Bhabha National Institute, Training School Complex, Anushakti Nagar, Mumbai
400094, INDIA.*

[§]*Fuel Chemistry Division, Indira Gandhi Centre for Atomic Research, Kalpakkam 603102,
INDIA*

AUTHOR INFORMATION

Corresponding Author

*Email: tapang@barc.gov.in; Fax: 0091-22-25505151

List of Figures

Figure S1: Variation in the potential energy with the change in the temperature at different time steps of (a) Lu@Pb_{12}^+ , (b) Lu@Pb_{12} , (c) Lu@Pb_{12}^- and (d) Lu@Pb_{12}^{2-} clusters in simulated annealing molecular dynamics.

Figure S2. The variation of density of states (DOS) as a function of molecular orbital energies of bare Sn_{12}^{2-} cluster, Lr^{3+} and Lu^{3+} metal ion encapsulated Sn_{12}^{2-} clusters as obtained by PBE/DEF level of theory. (Vertical green arrow is pointing toward HOMO.)

Figure S3. Molecular orbital energy level diagrams of bare Sn_{12}^{2-} cluster, Lr^{3+} and Lu^{3+} metal ion encapsulated Sn_{12}^{2-} clusters as obtained by B3LYP/DEF level of theory. (The HOMO energy of Sn_{12}^{2-} is scaled with the HOMO energy of Lr@Sn_{12}^+ cluster.)

Figure S4. Molecular orbital energy level diagrams of (a) bare Pb_{12}^{2-} cluster, Lr^{3+} and Lu^{3+} metal ion encapsulated Pb_{12}^{2-} clusters (b) bare Sn_{12}^{2-} cluster, Lr^{3+} and Lu^{3+} metal ion encapsulated Sn_{12}^{2-} clusters as obtained by PBE/DEF level of theory. (The HOMO energy of Pb_{12}^{2-} and Sn_{12}^{2-} is scaled with the HOMO energy of Lr@Pb_{12}^+ and Lr@Sn_{12}^+ cluster, respectively.)

Figure S5. The 2-D color-filled maps of electron localization function (ELF) of the endohedral clusters for Lr@Sn_{12}^+ and Lu@Sn_{12}^+ , respectively, using Multiwfn software as obtained by PBE method using small core ECP along with electron density function (EDF).

Figure S6. Vibrational frequency plots of (a) bare Pb_{12}^{2-} cluster, Lr^{3+} and Lu^{3+} metal ion encapsulated Pb_{12}^{2-} clusters, (b) bare Sn_{12}^{2-} cluster, Lr^{3+} and Lu^{3+} metal ion encapsulated Sn_{12}^{2-} clusters as obtained by PBE/DEF level of theory.

Figure S7. Scalar relativistic (left panel) and spin orbit splitting (right panel) of the valence molecular orbital energy levels for (a) Bare Sn_{12}^{2-} , (b) Lr@Sn_{12}^+ and (c) Lu@Sn_{12}^+ , clusters as obtained by B3LYP/TZ2P level of theory. (The HOMO energy of Sn_{12}^{2-} is scaled with the HOMO energy of Lr@Sn_{12}^+ cluster.)

Figure S8. Scalar relativistic (left panel) and spin orbit splitting (right panel) of the valence molecular orbital energy levels for (a) Bare Pb_{12}^{2-} , (b) Lr@Pb_{12}^+ and (c) Lu@Pb_{12}^+ , clusters as obtained by PBE/TZ2P level of theory. (The HOMO energy of Pb_{12}^{2-} is scaled with the HOMO energy of Lr@Pb_{12}^+ cluster.)

Figure S9. Scalar relativistic (left panel) and spin orbit splitting (right panel) of the valence molecular orbital energy levels for (a) Bare Sn_{12}^{2-} , (b) Lr@Sn_{12}^+ and (c) Lu@Sn_{12}^+ , clusters as obtained by PBE/TZ2P level of theory. (The HOMO energy of Sn_{12}^{2-} is scaled with the HOMO energy of Lr@Sn_{12}^+ cluster.)

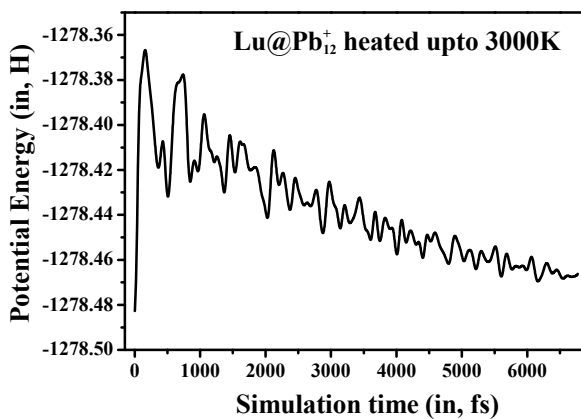
List of Tables

Table S1. Calculated Values of M–Pb/M–Sn and Pb–Pb/Sn–Sn Bond Critical Point Electron Density (ρ in $e a_0^{-3}$), Laplacian of Electron Density ($\nabla^2\rho$ in $e a_0^{-5}$), Local Electron Energy Density (E_d in au), and Ratio of Local Electron Kinetic Energy Density and Electron Density ($G(r)/\rho$ in au) and ELF Value of La@Pb_{12}^+ Cluster as obtained by using PBE Method with Large^a and Small^b Core ECP, and All Electron Basis Set^c. EDF has been Employed for Calculations with ECP Basis Sets.

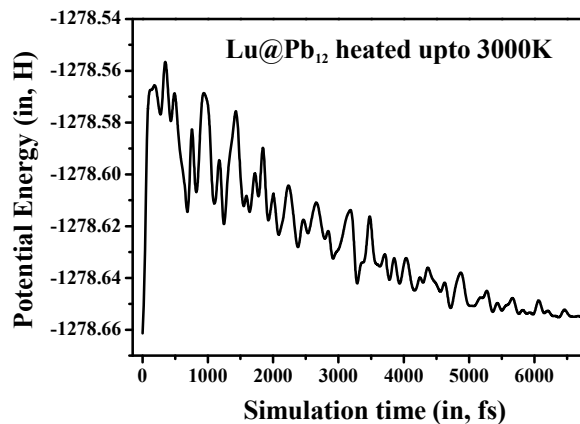
Table S2. Calculated Values of Average M–Pb/M–Sn Distances ($R_{(M-Pb/M-Sn)}$, in Å), Pb–Pb/Sn–Sn Distances ($R_{(Pb-Pb/Sn-Sn)}$, in Å), Binding Energy (BE, in eV), and HOMO–LUMO Energy Gap (ΔE_{Gap} , in eV) of Pb_{12}^{2-} , Sn_{12}^{2-} and Most Stable Isomer of M@Pb_{12}^{2-} and M@Sn_{12}^{2-} ($M = \text{Lr}^{3+}$, Lu^{3+} , La^{3+} and Ac^{3+}) Clusters obtained by using PBE^{b,c} Method along with Small Core ECP.

Table S3. Calculated Values of M–Pb/M–Sn and Pb–Pb/Sn–Sn Bond Critical Point Electron Density (ρ in $e a_0^{-3}$), Laplacian of Electron Density ($\nabla^2\rho$ in $e a_0^{-5}$), Local Electron Energy Density (E_d in au), and Ratio of Local Electron Kinetic Energy Density and Electron Density ($G(r)/\rho$ in au) and ELF Value of M@Pb_{12}^{2-} and M@Sn_{12}^{2-} ($M = \text{Lr}^{3+}$, Lu^{3+} , La^{3+} and Ac^{3+}) Clusters as obtained by using PBE^a Method along with Small Core ECP Employed with EDF.

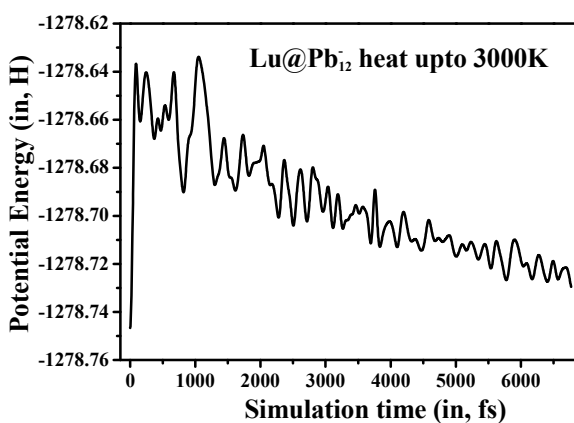
Table S4. Calculated Harmonic Vibrational Frequencies (in cm^{-1}) and Intensities (in km mol^{-1} as given in Parenthesis) of Pb_{12}^{2-} , Sn_{12}^{2-} , M@Pb_{12}^{2-} and M@Sn_{12}^{2-} ($M = \text{Lr}^{3+}$ and Lu^{3+}) Clusters as Obtained by using PBE/DEF Method.



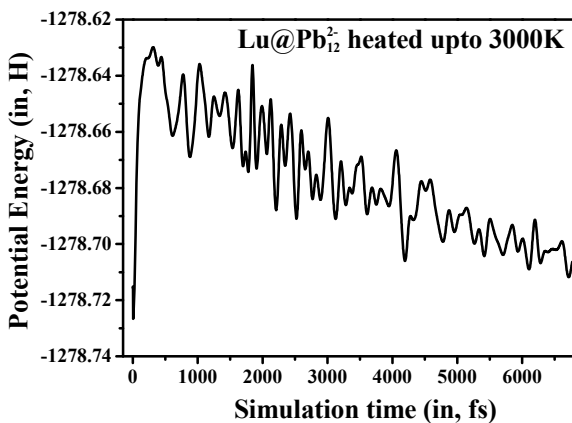
(a)



(b)



(c)



(d)

Figure S1: Variation in the potential energy with the change in the temperature at different time steps of (a) Lu@Pb₁₂⁺, (b) Lu@Pb₁₂, (c) Lu@Pb₁₂⁻ and (d) Lu@Pb₁₂²⁻ clusters in simulated annealing molecular dynamics.

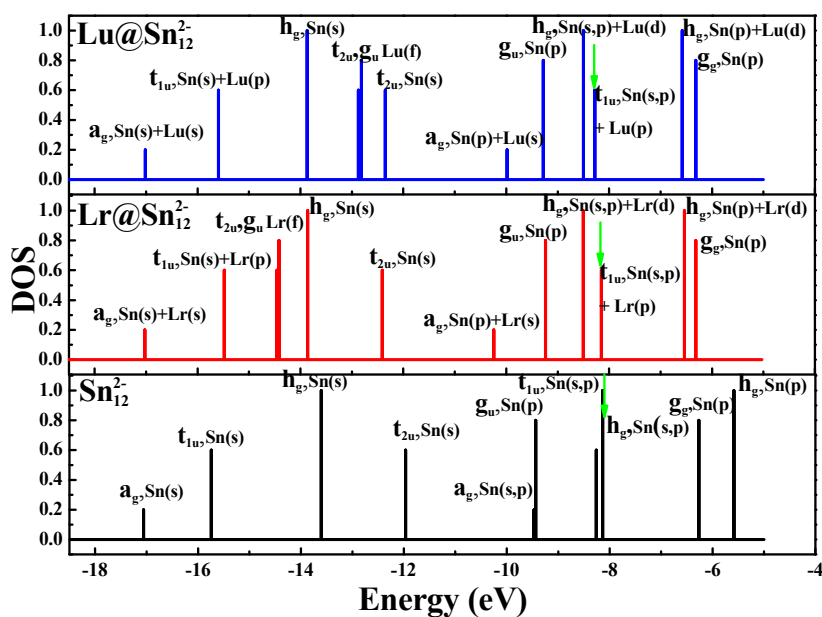


Figure S2. The variation of density of states (DOS) as a function of molecular orbital energies of bare Sn_{12}^{2-} cluster, Lr^{3+} and Lu^{3+} metal ion encapsulated Sn_{12}^{2-} clusters as obtained by PBE/DEF level of theory. (Vertical green arrow is pointing toward HOMO.)

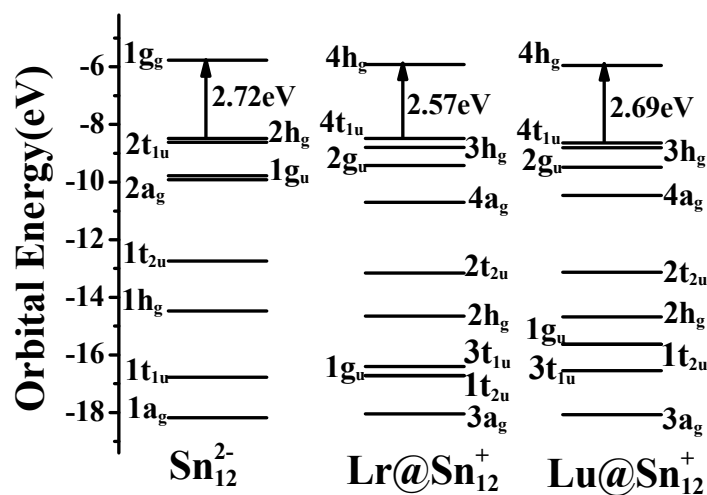
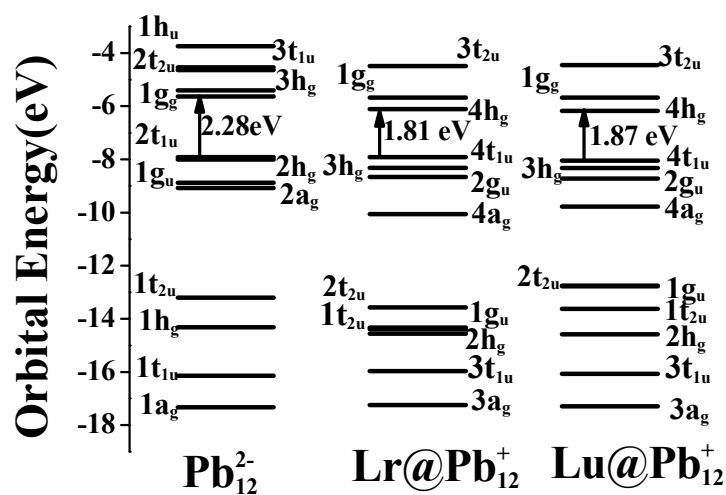
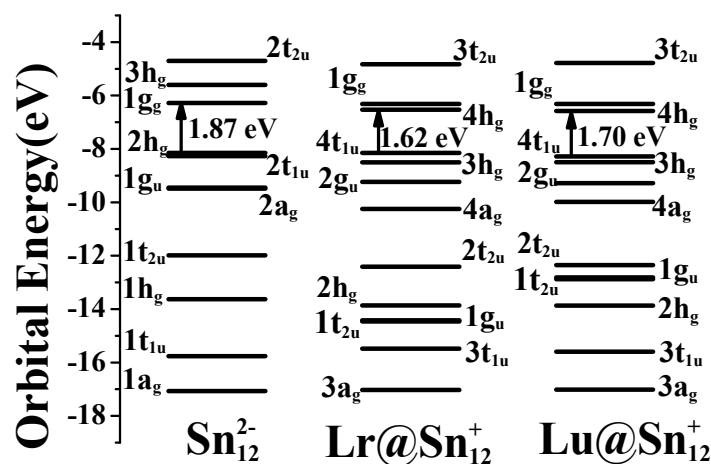


Figure S3. Molecular orbital energy level diagrams of bare Sn_{12}^{2-} cluster, Lr^{3+} and Lu^{3+} metal ion encapsulated Sn_{12}^{2-} clusters as obtained by B3LYP/DEF level of theory. (The HOMO energy of Sn_{12}^{2-} is scaled with the HOMO energy of Lr@Sn_{12}^{+} cluster.)

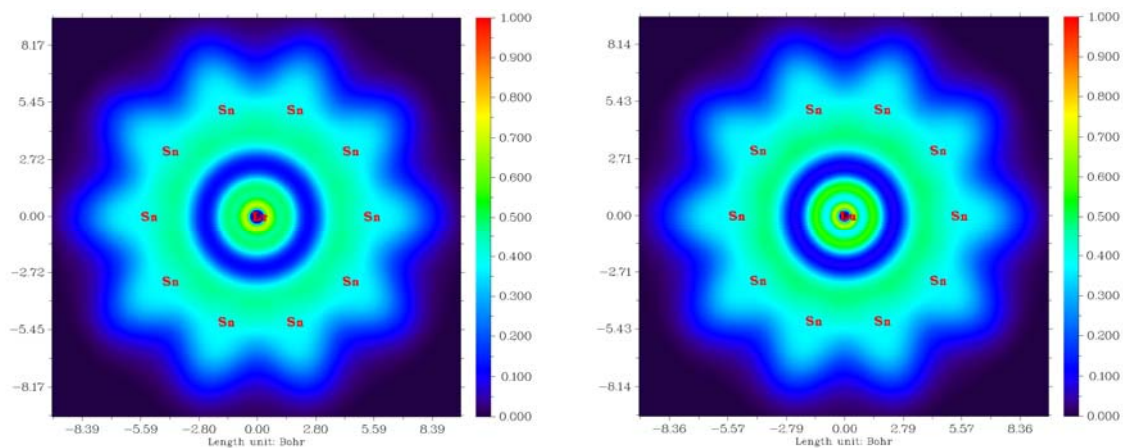


(a)



(b)

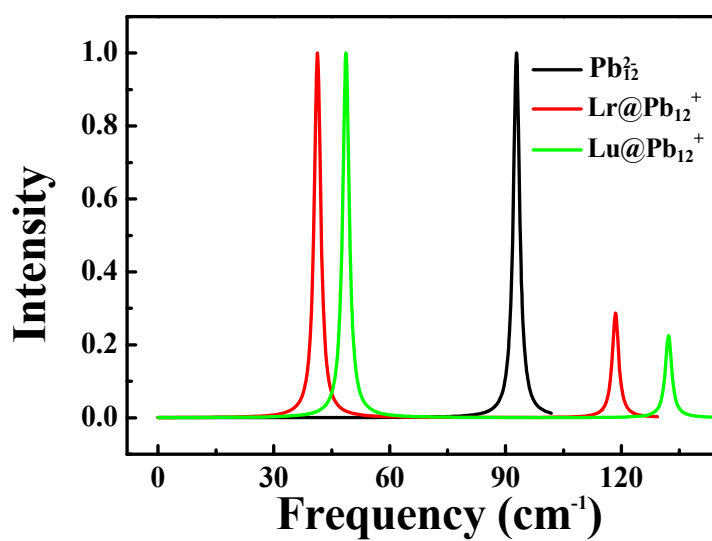
Figure S4. Molecular orbital energy level diagrams of (a) bare Pb_{12}^{2-} cluster, Lr^{3+} and Lu^{3+} metal ion encapsulated Pb_{12}^{2-} clusters (b) bare Sn_{12}^{2-} cluster, Lr^{3+} and Lu^{3+} metal ion encapsulated Sn_{12}^{2-} clusters as obtained by PBE/DEF level of theory. (The HOMO energy of Pb_{12}^{2-} and Sn_{12}^{2-} is scaled with the HOMO energy of Lr@Pb_{12}^{+} and Lr@Sn_{12}^{+} cluster, respectively.)



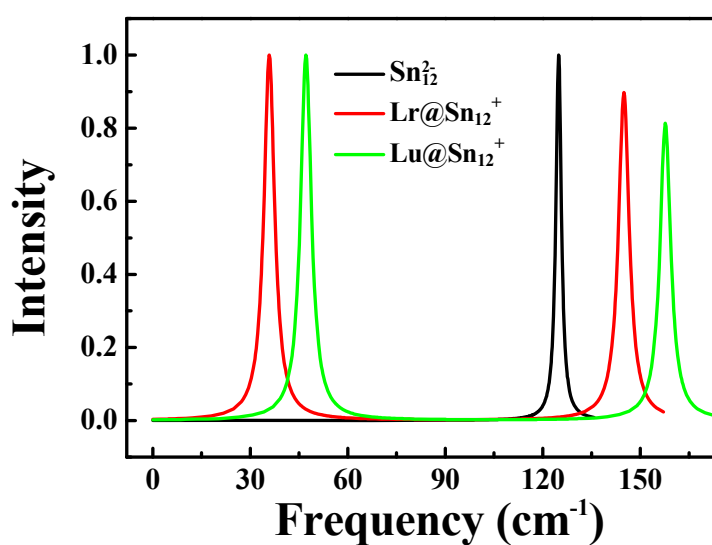
(a)

(b)

Figure S5. The 2-D color-filled maps of electron localization function (ELF) of the endohedral clusters for (a) Lr@Sn_{12}^+ and (b) Lu@Sn_{12}^+ , respectively, using Multiwfn software as obtained by PBE method using small core ECP along with electron density function (EDF).



(a)



(b)

Figure S6. Vibrational frequency plots of (a) bare Pb₁₂²⁻ cluster, Lr³⁺ and Lu³⁺ metal ion encapsulated Pb₁₂²⁻ clusters, (b) bare Sn₁₂²⁻ cluster, Lr³⁺ and Lu³⁺ metal ion encapsulated Sn₁₂²⁻ clusters as obtained by PBE/DEF level of theory.

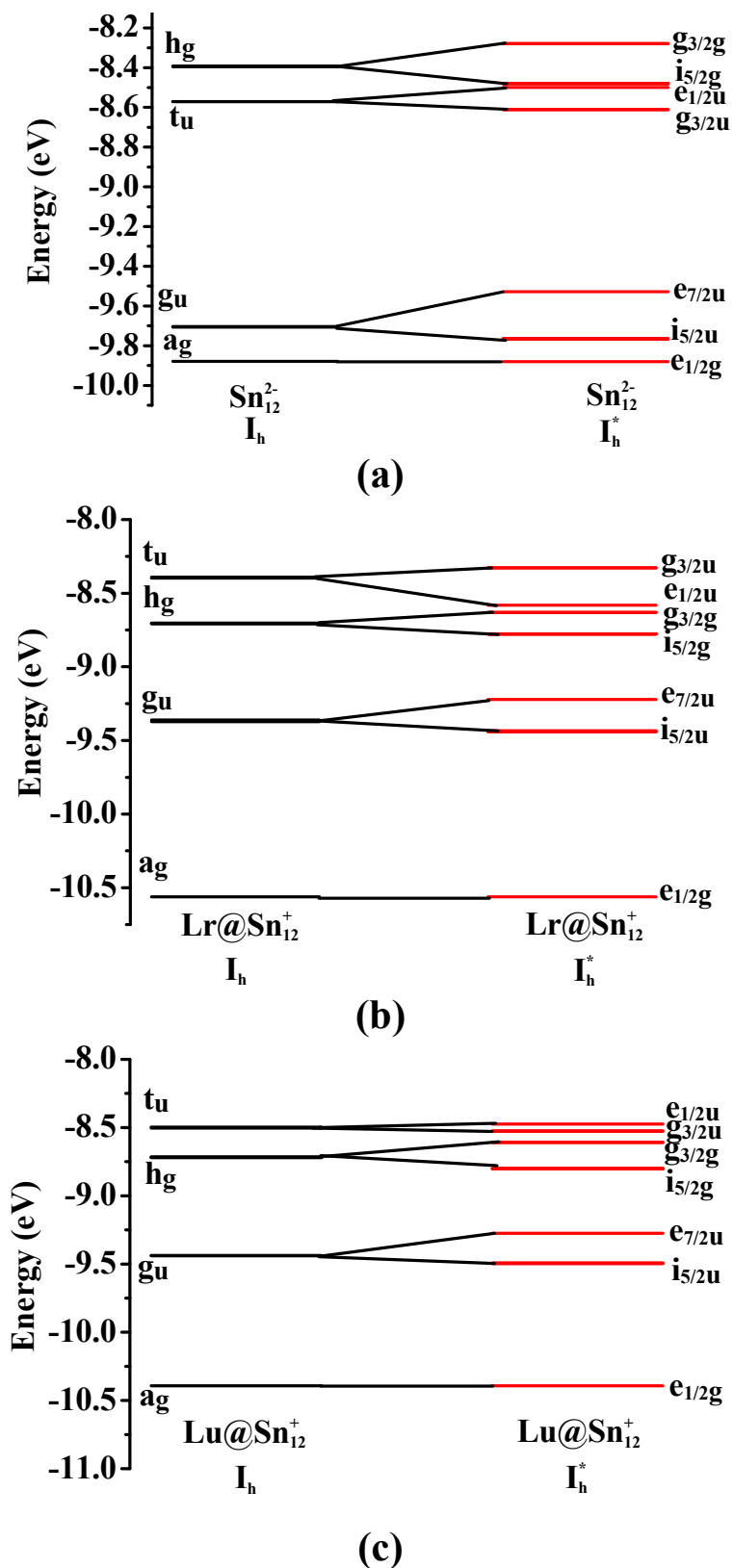


Figure S7. Scalar relativistic (left panel) and spin orbit splitting (right panel) of the valence molecular orbital energy levels for (a) Bare Sn_{12}^{2-} , (b) Lr@Sn_{12}^+ and (c) Lu@Sn_{12}^+ , clusters as obtained by B3LYP/TZ2P level of theory. (The HOMO energy of Sn_{12}^{2-} is scaled with the HOMO energy of Lr@Sn_{12}^+ cluster.)

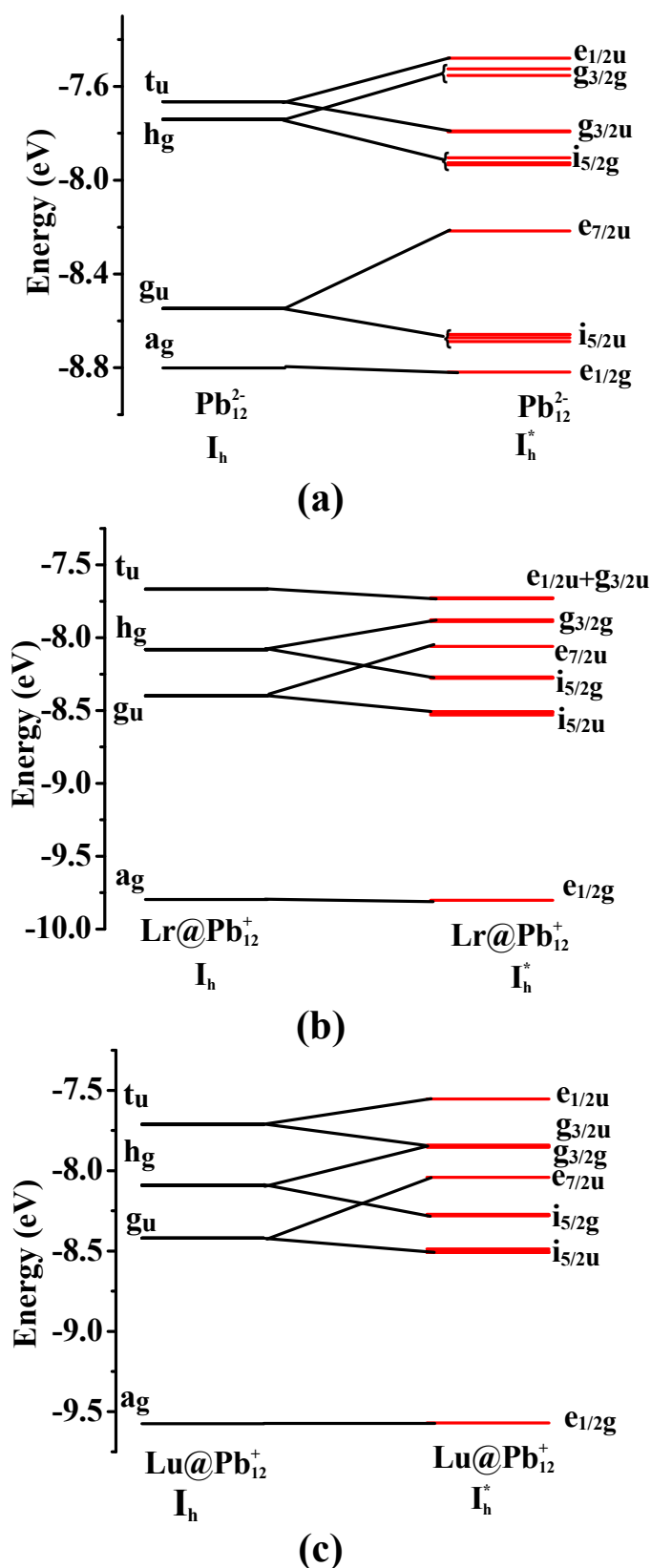
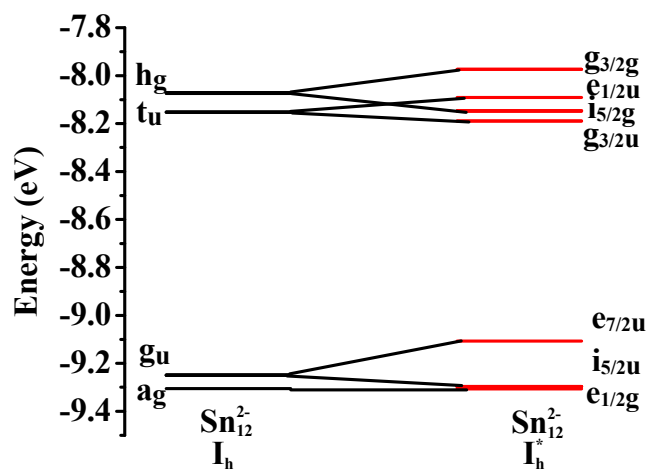
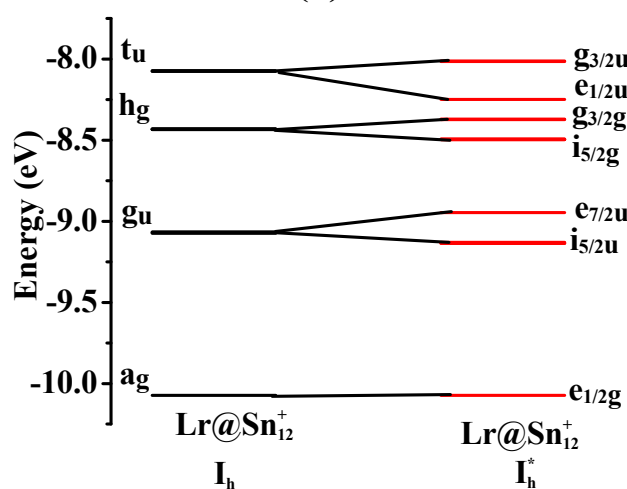


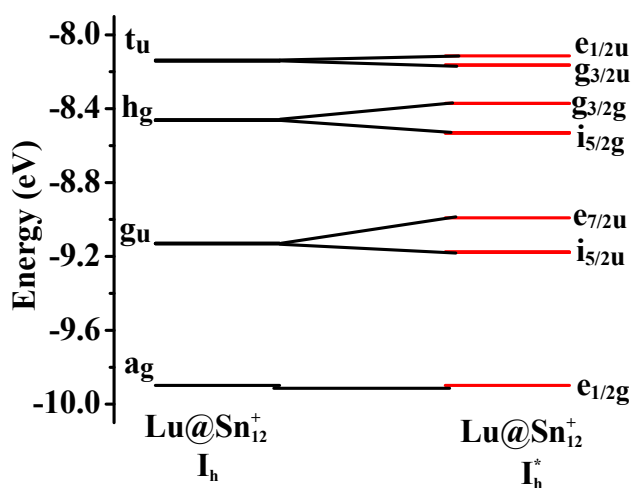
Figure S8. Scalar relativistic (left panel) and spin orbit splitting (right panel) of the valence molecular orbital energy levels for (a) Bare Pb_{12}^{2-} , (b) Lr@Pb_{12}^{+} and (c) Lu@Pb_{12}^{+} , clusters as obtained by PBE/TZ2P level of theory. (The HOMO energy of Pb_{12}^{2-} is scaled with the HOMO energy of Lr@Pb_{12}^{+} cluster.)



(a)



(b)



(c)

Figure S9. Scalar relativistic (left panel) and spin orbit splitting (right panel) of the valence molecular orbital energy levels for (a) Bare Sn_{12}^{2-} , (b) Lr@Sn_{12}^+ and (c) Lu@Sn_{12}^+ , clusters as obtained by PBE/TZ2P level of theory. (The HOMO energy of Sn_{12}^{2-} is scaled with the HOMO energy of Lr@Sn_{12}^+ cluster.)

Table S1. Calculated Values of M–Pb/M–Sn and Pb–Pb/Sn–Sn Bond Critical Point Electron Density (ρ in $e a_0^{-3}$), Laplacian of Electron Density ($\nabla^2\rho$ in $e a_0^{-5}$), Local Electron Energy Density (E_d in au), and Ratio of Local Electron Kinetic Energy Density and Electron Density ($G(r)/\rho$ in au) and ELF Value of La@Pb_{12}^+ Cluster as obtained by using PBE Method with Large^a and Small^b Core ECP, and All Electron Basis set^c. EDF has been employed for calculations with ECP basis sets.

Cluster	Bond	ρ	$\nabla^2\rho$	$G(r)^b$	$V(r)^c$	$E_d(r)/H(r)$	$G(r)/\rho$	Type ^d	ELF
^a La@Pb_{12}^+	La–Pb	0.015	0.032	0.009	–0.009	–0.001	0.600	C, D	0.084
	Pb–Pb	0.016	0.009	0.004	–0.004	–0.001	0.250	C, D	0.420
^b La@Pb_{12}^+	La–Pb	0.022	0.051	0.014	–0.016	–0.001	0.647	C, D	0.108
	Pb–Pb	0.022	0.018	0.006	–0.008	–0.002	0.286	C, D	0.387
^c La@Pb_{12}^+	La–Pb	0.024	0.047	0.014	–0.016	–0.002	0.585	C, D	0.141
	Pb–Pb	0.025	0.010	0.006	–0.010	–0.004	0.244	C, D	0.499

^adef–TZVP and def2–TZVP basis sets with large core for Pb(78) and La(46), respectively.

^bdef2–TZVP and Stuttgart basis sets with small core for Pb(60) and La(28), respectively.

^cAll electron UGBS basis set for La and Pb.

Table S2. Calculated Values of Average M–Pb/M–Sn Distances ($R_{(M-Pb/M-Sn)}$, in Å), Pb–Pb/Sn–Sn Distances ($R_{(Pb-Pb/Sn-Sn)}$, in Å), Binding Energy (BE, in eV), and HOMO–LUMO Energy Gap (ΔE_{Gap} , in eV) of Pb_{12}^{2-} , Sn_{12}^{2-} and Most Stable Isomer of $M@Pb_{12}^{2-}$ and $M@Sn_{12}^{2-}$ ($M = Lr^{3+}$, Lu^{3+} , La^{3+} and Ac^{3+}) Clusters obtained by using PBE^{b,c} Method along with Small Core ECP.

Cluster	Geometry	$R_{(M-Pb/M-Sn)}$	$R_{(Pb-Pb/Sn-Sn)}$	BE	ΔE_{Gap}
^a Pb_{12}^{2-}	I_h	3.086	3.244	...	2.150
^a Sn_{12}^{2-}	I_h	2.968	3.121	...	1.930
^b $Lr@Pb_{12}^+$	Str1(I_h)	3.258	3.426	–37.724	1.683
^b $Lu@Pb_{12}^+$	Str1(I_h)	3.239	3.405	–38.419	1.746
^b $Lr@Sn_{12}^+$	Str1(I_h)	3.159	3.321	–36.402	1.591
^b $Lu@Sn_{12}^+$	Str1(I_h)	3.139	3.300	–37.201	1.670
^c $La@Pb_{12}^+$	Str1(I_h)	3.337	3.509	–32.259	1.148
^b $Ac@Pb_{12}^+$	Str1(I_h)	3.392	3.567	–29.363	1.108

^aIn the case of Pb_{12}^{2-} and Sn_{12}^{2-} , $R_{(M-Pb/M-Sn)}$ refers to the distance from the centre to the cage atoms.

^bdef–TZVP basis set with small core for Lr (ECP 60), Ac (ECP 60), Lu (ECP 28) and def2–TZVP basis set with small core for Pb (ECP 60), Sn (ECP 28).

^cStuttgart basis set with small core for La (ECP 28) and def2–TZVP basis set with small core for Pb (ECP 60).

Table S3. Calculated Values of M–Pb/M–Sn and Pb–Pb/Sn–Sn Bond Critical Point Electron Density (ρ in $e a_0^{-3}$), Laplacian of Electron Density ($\nabla^2\rho$ in $e a_0^{-5}$), Local Electron Energy Density (E_d in au), and Ratio of Local Electron Kinetic Energy Density and Electron Density ($G(r)/\rho$ in au) and ELF Value of $M@Pb_{12}^{2-}$ and $M@Sn_{12}^{2-}$ ($M = Lr^{3+}, Lu^{3+}, La^{3+}$ and Ac^{3+}) Clusters as obtained by using PBE^a Method along with Small Core ECP Employed with EDF.

Cluster	Bond	ρ	$\nabla^2\rho$	$G(r)^b$	$V(r)^c$	$E_d(r)/H(r)$	$G(r)/\rho$	Type ^d	ELF
$Lr@Pb_{12}^+$	Lr–Pb	0.023	0.039	0.013	–0.016	–0.003	0.541	C, D	0.158
	Pb–Pb	0.023	0.021	0.007	–0.009	–0.002	0.318	C, D	0.343
$Lu@Pb_{12}^+$	Lu–Pb	0.022	0.037	0.012	–0.015	–0.003	0.541	C, D	0.147
	Pb–Pb	0.023	0.022	0.008	–0.010	–0.002	0.325	C, D	0.341
$Lr@Sn_{12}^+$	Lr–Sn	0.026	0.041	0.014	–0.018	–0.004	0.542	C, D	0.178
	Sn–Sn	0.025	0.015	0.007	–0.010	–0.003	0.271	C, D	0.456
$Lu@Sn_{12}^+$	Lu–Sn	0.024	0.041	0.014	–0.017	–0.003	0.557	C, D	0.158
	Sn–Sn	0.026	0.016	0.007	–0.010	–0.003	0.275	C, D	0.453
$La@Pb_{12}^+$	La–Pb	0.022	0.051	0.014	–0.016	–0.001	0.647	C, D	0.108
	Pb–Pb	0.022	0.018	0.006	–0.008	–0.002	0.286	C, D	0.387
$Ac@Pb_{12}^+$	Ac–Pb	0.021	0.045	0.013	–0.014	–0.001	0.611	C, D	0.111
	Pb–Pb	0.020	0.015	0.005	–0.008	–0.002	0.259	C, D	0.399

^adef–TZVP basis set with small core for Lr (ECP 60), Ac (ECP 60), Lu (ECP 28), def2–TZVP basis set with small core for Pb (ECP 60), Sn (ECP 28) and Stuttgart basis set with small core for La (ECP 28).

^b $G(r)$ represents the local electron kinetic energy density.

^c $V(r)$ signifies the local electron potential energy density.

^d“Type” is an indication of type of very weak covalent interaction exists in between the corresponding pair of bonding atoms.

Table S4. Calculated Harmonic Vibrational Frequencies (in cm^{-1}) and Intensities (in km mol^{-1} as given in Parenthesis) of Pb_{12}^{2-} , Sn_{12}^{2-} , M@Pb_{12}^{2-} and M@Sn_{12}^{2-} ($\text{M} = \text{Lr}^{3+}$ and Lu^{3+}) Clusters as Obtained by using PBE/DEF Method.

Pb_{12}^{2-}	Sn_{12}^{2-}	Lr@Pb_{12}^{+}	Lu@Pb_{12}^{+}	Lr@Sn_{12}^{+}	Lu@Sn_{12}^{+}
51.51 (0.0) (h_u)	66.97 (0.0) (h_u)	40.34 (0.0) (h_u)	41.52 (0.0) (h_u)	35.85 (5.82) (t_{1u})	47.13 (6.09) (t_{1u})
53.26 (0.0) (h_g)	72.70 (0.0) (h_g)	41.30 (4.04) (t_{1u})	48.68 (4.36) (t_{1u})	50.40 (0.0) (h_u)	51.93 (0.0) (h_u)
70.97 (0.0) (g_g)	93.72 (0.0) (g_g)	58.70 (0.0) (g_g)	60.25 (0.0) (g_g)	73.95 (0.0) (g_u)	76.52 (0.0) (g_g)
75.44 (0.0) (t_{2u})	102.62 (0.0) (t_{2u})	62.39 (0.0) (h_g)	64.09 (0.0) (h_g)	74.36 (0.0) (g_g)	78.06 (0.0) (g_u)
83.35 (0.0) (g_u)	111.11 (0.0) (g_u)	63.74 (0.0) (g_u)	66.35 (0.0) (g_u)	80.32 (0.0) (h_g)	83.08 (0.0) (h_g)
89.59 (0.0) (h_g)	118.54 (0.0) (h_g)	84.08 (0.0) (t_{2u})	83.30 (0.0) (t_{2u})	115.15 (0.0) (h_g)	113.96 (0.0) (t_{2u})
89.30 (0.0) (a_g)	122.59 (0.0) (a_g)	85.56 (0.0) (h_g)	86.40 (0.0) (a_g)	115.45 (0.0) (t_{2u})	115.87 (0.0) (h_g)
92.84 (0.05) (t_{1u})	124.88 (0.10) (t_{1u})	90.17 (0.0) (a_g)	90.90 (0.0) (a_g)	120.67 (0.0) (a_g)	121.79 (0.0) (a_g)
...	...	118.48(1.16) (t_{1u})	132.21 (0.98) (t_{1u})	144.96 (5.22) (t_{1u})	157.72 (4.95) (t_{1u})